

AD-A093 455

CAMBRIDGE ACOUSTICAL ASSOCIATES INC MA
HIGH FREQUENCY ASYMPTOTICS AND THE TRANSITION MATRIX FORMULATIO--ETC(U)
FEB 80 J M GARRELICK
CAA-U-659-260

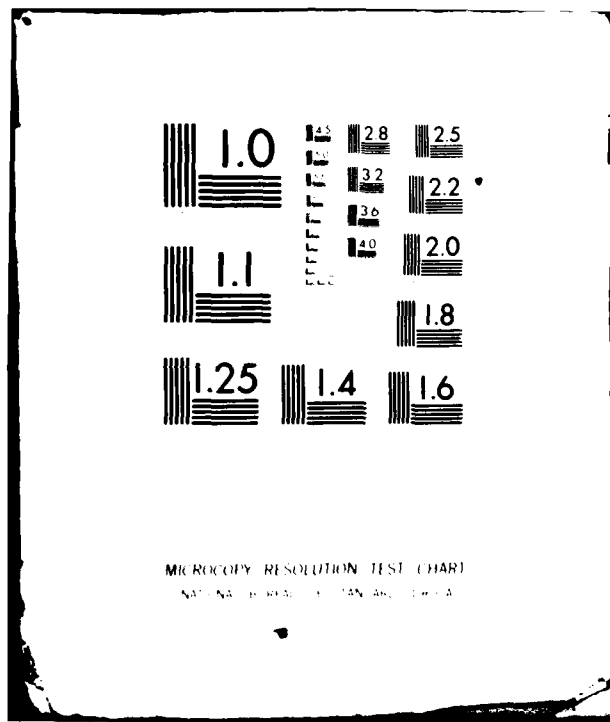
F/6 20/1
N00014-78-C-0218
NL

UNCLASSIFIED

| - |
A-99216



END
CATF
FILED
2 81
DTIC



MICROCOPY RESOLUTION TEST CHART

NATIONAL BUREAU OF STANDARDS 1963

AD A093455

LEVEL 1

CAMBRIDGE
ACOUSTICAL
ASSOCIATES

HIGH FREQUENCY ASYMPTOTICS AND THE TRANSITION
MATRIX FORMULATION OF SCATTERING

Prepared by:
Joel M. Garrellick

February 1980

DTIC
JAN 2 1981
D

Report U-659-260

Prepared for:
Office of Naval Research
Structural Mechanics Program
Arlington, Virginia 22217
Contract N00014-78-C-0218

DISTRIBUTION STATEMENT A
Approved for public release;
Distribution Unlimited

DDC FILE COPY

64 RINDGE AVENUE EXT., CAMBRIDGE, MASSACHUSETTS 02140

80 10 31 013

①

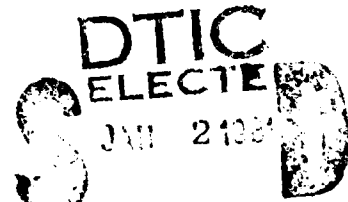
⑥ HIGH FREQUENCY ASYMPTOTICS AND THE
TRANSITION MATRIX FORMULATION OF SCATTERING

Prepared by:

⑩ Joel M. Garrellick

⑫ 311

⑪ Feb. [redacted] 80



C

⑬ CAA-U-659-260

Report U-659-260
Prepared for Office of Naval Research

Structural Mechanics Program

Arlington, Virginia 22217

Contract N00014-78-C-0218 [redacted]

⑮

DISTRIBUTION STATEMENT A

Approved for public release;
Distribution Unlimited

Cambridge Acoustical Associates, Inc.
54 Rindge Avenue Extension
Cambridge, Massachusetts 02140

072750

JOB

TABLE OF CONTENTS

	<u>Page</u>
ABSTRACT	iii
I. INTRODUCTION	1
II. ELASTIC SCATTERING FROM SPHERICAL INCLUSIONS	
A. Governing Equations of Motion	3
B. Formulations for Solution	
1. Wave Harmonics	4
2. Creeping Waves	6
3. Physical Optics; Kirchhoff	9
4. T-Matrix	11
III. THE USE OF HIGH FREQUENCY ASYMPTOTICS TO EVALUATE AND FACILITATE THE CONVERGENCE OF T-MATRIX SOLUTIONS	
A. General Formulation	14
B. Illustrative Examples	
1. Spherical Cavity	16
2. Prolate Spheriodal Cavity	16
REFERENCES	19-21
FIGURES	22-27

Accession For	
NTIS GRA&I	<input checked="" type="checkbox"/>
DTIC TAB	<input type="checkbox"/>
Unannounced	<input type="checkbox"/>
Justification	
for FL- 182 - file	
By _____	
Distribution/	
Availability Codes	
Air-Int and/or	
Distr	Special
<i>A</i>	

ABSTRACT

This report deals with the use of high frequency asymptotics to evaluate and possibly facilitate, the convergence of the transition matrix formulation of scattering. For illustrative purposes, elastic and acoustic scattering from spherical and spheroidal cavities is considered in some detail. References are presented for other types of inclusions. Finally, a general method is suggested for integrating high frequency asymptotic solutions into the T-matrix formulation itself with the purpose of improving convergence. The method is implemented for the case of a spherical, and a prolate spheroidal, cavity.

I. INTRODUCTION

The transition matrix (T-matrix) formulation of scattering is the most recent addition to the well-known classical methods: separation of variables, the integral equation method, and the variational method.^{1,2} This method has been applied to acoustic, elastic, and electromagnetic media and to a variety of complicated geometries.²⁻⁶

All of the above methods, including the T-matrix method, have the drawback of poor convergence when the ratio $D/\lambda \gg 1$, where D is the characteristic dimension of the scatterer and λ is the characteristic wavelength of the scattered field. Typically, the number of terms required for convergence is of order $2D/\lambda$. However, "coordinate stretching" can be used to reduce the extent of the calculations implied by this criterion.⁷ While the TM method appears to be a most efficient formulation, and consequently, the most widely studied over these last few years, it too entails numerical difficulties at high frequencies.

For problems in steady state elastic and acoustic scattering, the character and functional dependence of the scattered field, as well as its amplitude, vary with frequency. In the low frequency or Rayleigh region, defined by $D/\lambda < 1$, the scattered field is completely defined in terms of only the gross characteristics of the scatterer, viz. its overall dimensions, relative density and compressibility.⁸ Computationally, this region generally involves little difficulty using any of the traditional analytical techniques. The low frequency regime is followed by the resonance, or standing wave, region whereby the scatterer dimensions are comparable to the characteristic wavelength(s), i.e., $D/\lambda = 0(1-10)$. It is at the upper end of this regime where numerical formulations, either modal or integral, begin to exhibit some computational difficulty; lack of convergence, round off errors, the existence of forbidden frequencies, etc.

As frequency increases further, or correspondingly as wavelength decreases, the scatterer begins to measure many wavelengths. Here the scattered field is more conveniently described in terms of travelling waves which are generated at the boundary of, and within, the scatterer. These travelling waves, because of diffraction and dissipation are attenuated as they circumnavigate the scatterer. For present purposes this is defined as the creeping wave region.* Finally, the limiting high frequency asymptotic (Kirchhoff or Physical Optics) region is defined as that region where ray theory applies, i.e., where the scatterer can be considered to be locally reacting and where each scattering element acts as if it were in an infinite baffle.

It is in these latter two frequency regimes where the computational difficulties encountered by numerical formulations, including the T matrix, become severe. The purpose of this study is to analyze the potential role that high frequency asymptotic scattering formulations may play in serving (a) as a convergence check for T matrix solutions, and (B) as a means for improving the convergence of T matrix formulations. For discussion purposes only elastic and acoustic media, and spherical or spheroidal scatterers, are considered. Also, the high frequency formulations are limited to the Kirchhoff and creeping wave type.

In Section II the problem of elastic scattering from spherical inclusions is reviewed, together with the corresponding T-matrix and wave harmonic formulations. The corresponding high frequency asymptotic solutions are also discussed in Section II. In Section III a general formalism for using these high frequency solutions to complement the T-matrix formulation is presented together with illustrative examples. Specifically, the examples are scalar scattering from a spherical, and a prolate spheroidal cavity.

* It is noted that this definition of the creeping wave region is more restrictive than need be since, in theory, creeping wave solutions can be as general as is the corresponding wave harmonic series from which they are derived.

II. ELASTIC SCATTERING FROM SPHERICAL INCLUSIONS

A. Governing Equations of Motion

The harmonic response of a three dimensional linearly elastic solid can be fully defined in terms of a scalar and a vector potential which satisfy a scalar and vector wave equation respectively. In spherical coordinates (Fig. 1), the vector wave equation is itself separable and one is left with the following governing equations of motion

$$c_d^2 \nabla^2 \phi + \omega^2 \phi = 0 \quad (1a)$$

$$c_s^2 \nabla^2 \psi + \omega^2 \psi = 0 \quad (1b)$$

$$c_s^2 \nabla^2 \chi + \omega^2 \chi = 0 \quad (1c)$$

from which the associated displacement field may be calculated. Using spherical coordinates⁹

$$u_r = \frac{\partial \phi}{\partial r} + a \frac{\partial^2 (r\chi)}{\partial r^2} - r \nabla^2 \chi \quad ; \quad (2a)$$

$$u_\theta = \frac{1}{r} \frac{\partial \phi}{\partial \theta} + \frac{1}{r \sin \theta} \frac{\partial (r\psi)}{\partial \beta} + a \frac{1}{r} \frac{\partial^2 (r\chi)}{\partial \theta \partial r} \quad ; \quad (2b)$$

$$u_\beta = \frac{1}{r \sin \theta} \frac{\partial \phi}{\partial \beta} - \frac{1}{r} \frac{\partial (r\psi)}{\partial \theta} + a \frac{1}{r \sin \theta} \frac{\partial^2 (r\chi)}{\partial \beta \partial r} \quad . \quad (2c)$$

In the above equations ω is the circular frequency and c_d and c_s represent the dilatational and shear wave speeds, respectively. The corresponding stress field can also be explicitly determined.⁹ For an axisymmetric, i.e., β independent, problem such as is considered in this report, $\psi = 0$. In the case of a cavity of radius a centered at the origin the boundary conditions to be satisfied are

$$\sigma_{rr}(a, \theta, \beta) = \sigma_{r\theta}(a, \theta, \beta) = \sigma_{r\beta}(a, \theta, \beta) = 0 \quad (3a)$$

For a rigid and immovable inclusion, also of radius a and centered at the origin, the boundary conditions are

$$u_x(a, \theta, \beta) = u_\theta(a, \theta, \beta) = 0 \quad (3b)$$

A dilatational source may be represented by the potential

$$\begin{aligned} \phi^i(r, \theta) &= \phi_o \exp(ik_d R)/R \\ &= -i \phi_o k_d \sum_n (2n+1) h_n(k_d r_s) j_n(k_d r) P_n(\cos\theta) \end{aligned} \quad (4)$$

where $k_d = \omega/c_d$ and r_s and r refer to source and receiver locations respectively, with $r_s > 1$. The spherical Hankel and Bessel functions are denoted by $h_n(x)$ and $j_n(x)$, and $P_n(x)$ is the Legendre function. For $k_d r_s \gg 1$ the large argument asymptotic expression for the spherical Hankel function may be used and Eq. 4 reduces to the expansion for an incident plane wave

$$\phi^i(r, \theta) = \phi_o \sum_n (2n+1) i^n j_n(k_d r) P_n(\cos\theta) \quad (5)$$

with

$$\phi_o = \phi_o \exp(ik_d r_s)/r_s$$

Alternatively, a distortional (axisymmetric) source may be specified.

$$\begin{aligned} x^i(r, \theta) &= \chi_o k_s^2 r_s \sin\theta \exp(ik_s R)/R \\ &= -i \chi_o k_s \sum_n (2n+1) h_n(k_s r_s) j_n(k_s r) dP_n(\cos\theta)/d\theta \end{aligned} \quad (6)$$

where $k_s = \omega/c_s$. For this source the vibration is transverse, and in the incident plane at large distances.

B. Formulations for Solution

1. Wave Harmonics

Using spherical wave harmonics, the potentials which define the scattered field for the (axisymmetric) problems posed above are given in series form

$$\phi = \sum_n A_n h_n(k_d r) P_n(\cos\theta) \quad (7)$$

$$\chi = \sum_n B_n h_n(k_s r) dP_n(\cos\theta)/d\theta$$

The unknown coefficients A_n and B_n are determined from the appropriate boundary conditions and source configuration. For example, in the case of a dilatational source incident on a spherical cavity⁹

$$\begin{bmatrix} A_n \\ B_n \end{bmatrix} = \frac{-\phi_0 i^n (2n+1)}{D} \begin{bmatrix} a_{22} & -a_{12} \\ -a_{21} & a_{11} \end{bmatrix} \begin{bmatrix} b_1 \\ b_2 \end{bmatrix} \quad (8)$$

with

$$D = a_{11}a_{22} - a_{12}a_{21} \quad (9)$$

and where

$$\begin{aligned} a_{11} &= [n(n-1) - (k_s a)^2/2] h_n(k_d a) + 2(k_d a) h_{n+1}(k_d a) \\ a_{12} &= n(n+1) [(n-1)h_n(k_s a) - (k_s a)h_{n+1}(k_s a)] \\ a_{21} &= (n-1)h_n(k_d a) - (k_d a)h_{n+1}(k_d a) \\ a_{22} &= [n^2 - 1 - (k_s a)^2/2] h_n(k_s a) + (k_s a) h_{n+1}(k_s a) \\ b_1 &= [n(n-1) - (k_s a)^2/2] j_n(k_d a) + 2(k_d a) j_{n+1}(k_d a) \\ b_2 &= (n-1) j_n(k_d a) - (k_d a) j_{n+1}(k_d a) \end{aligned} \quad (10)$$

Substituting Eqs. 10 into Eq. 9

$$\begin{aligned} D &= \phi_1 h_n(k_d a) h_n(k_s a) + \phi_2 h_n(k_d a) h_{n+1}(k_s a) \\ &\quad + \phi_3 h_{n+1}(k_d a) h_n(k_s a) + \phi_4 h_{n+1}(k_d a) h_{n+1}(k_s a) \end{aligned} \quad (11)$$

with

$$\begin{aligned}
 \phi_1 &= (\kappa_s a)^2 / 2 \{ (2n+1)(n-1) - (\kappa_s a)^2 / 2 - 4n(n-1)(n^2-1) / (\kappa_s a)^2 \} \\
 \phi_2 &= (\kappa_s a) [n(n-1)(n+2) - (\kappa_s a)^2 / 2] \\
 \phi_3 &= (\kappa_d a) [(n^2-1)(n+2) - (\kappa_s a)^2] \\
 \phi_4 &= -(\kappa_d a)(\kappa_s a) [(n-1)(n+2)]
 \end{aligned} \tag{12}$$

Using the recursion relation

$$h_{n+1}(x) = \frac{n}{x} h_n(x) - d[h_n(x)]^2 / dx \tag{13}$$

The quantity D can also be expressed in the following form

$$\begin{aligned}
 D = & \bar{\phi}_1 h_n(\kappa_d a) h_n(\kappa_s a) + \bar{\phi}_2 h_n(\kappa_d a) h_n'(\kappa_s a) \\
 & + \bar{\phi}_3 h_n'(\kappa_d a) h_n(\kappa_s a) + \bar{\phi}_4 h_n'(\kappa_d a) h_n'(\kappa_s a)
 \end{aligned} \tag{14}$$

with

$$\begin{aligned}
 \bar{\phi}_1 &= n(n^2-1)(n+2) + (\kappa_s a)^4 / 4 - (\kappa_s a)^2 [2n(n+1)-1] / 2 \\
 \bar{\phi}_2 &= (\kappa_s a) [(\kappa_s a)^2 / 2] \\
 \bar{\phi}_3 &= (\kappa_s a) [(\kappa_s a)^2 - (n+2)(n-1)] \\
 \bar{\phi}_4 &= (\kappa_s a)(\kappa_d a) [2-n(n+1)]
 \end{aligned} \tag{15}$$

2. Creeping Waves

In general and including the results above, the wave harmonic formulation for elastic scattering can be shown to yield convergent series for the potentials as well as for the associated displacement and stress fields. However, it is the nature of the formulation that the number of terms required for convergence increases with frequency. In order to

transform such series into ones which converge rapidly at high frequencies, the Watson transformation is employed.¹⁰ A key ingredient in this transformation is the formula

$$\sum_n f(n+1/2) = (1/2) \int_C f(v) \exp(-iv) / \cos \pi v dv \quad (16)$$

where f is a reasonably well behaved function and C represents an appropriate contour. This contour is then deformed such that the integral can be evaluated in terms of a set of pole contributions, each representing a creeping wave. Specifically, for the class of problems considered here, this approach leads to the following identity

$$\begin{aligned} & \sum_{n=0}^{\infty} (2n+1) P_n(\cos \theta) f(n) / D(n) \\ &= 2\pi \sum_j \left\{ v P_{v-1/2}(\cos(\pi-\theta)) f(v-1/2) / [\cos v \pi \partial D(v-1/2) / \partial v] \right\}_{v=v_j} \end{aligned} \quad (17)$$

where the (creeping wave) roots v_j satisfy the equation

$$D(v_j - 1/2) = 0 \quad (18)$$

(It should be noted that Eq. 17 may also be obtained by means of the Poisson summation formula.¹¹)

For example, we again consider the case of a dilatational source incident on a spherical cavity. The solutions to Eq. 18, for $k_s a \gg 1$, are of three types.^{12,13} An infinite set of shear type

$$\pm v_{1j} (\Omega_s) \sim \Omega_s + 2^{-1/3} e^{5/3\pi i} (e^{-i\pi} z_j) \Omega_s^{1/2}, \quad j = 1, 2, 3, \dots, \quad (19)$$

An infinite set of dilatational type

$$\pm v_{2j} (\Omega_d) \sim \Omega_d + 2^{1/3} e^{5/3\pi i} (e^{i\pi} a_j) (\Omega_d)^{1/3}, \quad j = 1, 2, 3, \dots, \quad (20)$$

and a single pair of the Rayleigh type

$$\pm v_R \sim (c_s/c_R) \Omega_s \quad (21)$$

where the imaginary part of v_R vanishes exponentially as $\Omega_s \rightarrow \infty$. The z_j are the roots of $Ai(z)=0$ which are real and negative,¹⁴ $Ai(z)$ is the Airy function and c_R is the Rayleigh wave speed. It is interesting, as well as reassuring, to see that for high frequency scattering from a cavity there is a root $v_R \sim wa/c_R$ which corresponds to the Rayleigh surface wave on a (planar) half space.

The corresponding potentials (for $\theta \neq 0$) are given by^{13,15}

$$\begin{aligned} \phi_{c.w.} = & 2\pi i \exp(-i\pi/4) \Phi_0 \sum_s (-1)^s \sum_j v_j [j_{\bar{v}}(k_d r) \\ & + (\pi i/2) \exp(i\pi v_j) (a_{22} b_1 - a_{13} b_2)] \end{aligned} \quad (22)$$

$$\begin{aligned} h_{\bar{v}}(k_d r) / (\partial D / \partial v) \Big|_{n=\bar{v}} &= \sum_j P_{\bar{v}}(\cos\theta) \exp[i v_j (2\pi s + \pi/2)] \\ x_{c.w.} = & 2\pi i \exp(-i\pi/4) \Phi_0 \sum_s (-1)^s \sum_j v_j (\pi i/2) \exp(i\pi v_j) (a_{11} b_2 - a_{21} b_1) \\ h_{v_{j-1/2}}(k_s r) / (\partial D / \partial v) \Big|_{n=\bar{v}} &= \sum_j \frac{dP}{dv}(\cos\theta) / d\theta \end{aligned} \quad (23)$$

with $\bar{v} = v_j - 1/2$ and $\theta \neq 0$. The travelling, or creeping, wave nature of the above potentials is evident if one substitutes the large order asymptotic expressions for the Legendre functions in Eqs. 22 and 23.

$$P_{\bar{v}}(\cos\theta) \sim (2\pi v_j \sin\theta)^{-1/2} \{ \exp[i(v_j \theta - \pi/4)] + \exp[-i(v_j \theta - \pi/4)] \} \quad (24)$$

It can be shown that for large Ω_d and Ω_s the above series, as well as those for the corresponding displacements, converge as v_j^{-N} with $N \geq 1$ for $0 < \theta < \pi/2$ when $s=0$, and for $0 < \theta < \pi$ when $s \neq 1$.¹³ Thus, unlike the wave harmonic series given earlier the convergence of the creeping wave series actually improves with increasing frequency within their domain of validity. Also, convergence, improves with increasing θ . In other words, it improves as one moves away from the illuminated zone. This is a general phenomenon which in some cases limits the utility of creeping wave solutions to the shadow zone therefore providing a convenient supplement to physical optics solutions (Section II.B.3).

Creeping wave solutions exist for inclusions of other than spherical geometry and zero impedance as well as for other types of incident waves both harmonic and transient. Cylindrical cavities have been studied by Miklowitz¹⁶ and Peck¹⁷. Gaunaud and Uberall have obtained solutions to many different scattering problems including fluid filled spherical cavities embedded in a viscoelastic as well as elastic medium.^{18,19} (In their approach the contributions of creeping waves are represented in terms of Regge poles.) They have also considered incident waves of the distortional type.²⁰

3. Physical Optics; Kirchhoff

The physical optics, or Kirchhoff, high frequency asymptotic approach to scattering has been used extensively for radar²¹ and acoustic^{22,23} applications. The method is applicable to the illuminated zone and is most useful when applied to the specular return. The basis for this formulation is that each differential scatterer acts as though it were located in a planar infinite baffle. For the problem of elastic scattering, this assumption allows one to express the scattered potentials in terms of a Green's function which satisfies Neumann boundary conditions at the boundary of the scatterer.

$$\phi^S(\bar{R}) = -2 \int_{S_o} G_\phi(\bar{R}, \bar{R}_o) \partial \phi^2(\bar{R}_o)/\partial n \, dS_o \quad (25)$$

$$X^S(\bar{R}) = -2 \int_{S_o} G_X(\bar{R}, \bar{R}_o) \partial X^S(\bar{R}_o)/\partial n \, dS_o$$

with $G_\phi(\bar{R}, \bar{R}_o) = \exp(ik_d |\bar{R}-\bar{R}_o|)/[4\pi |\bar{R}-\bar{R}_o|]$ (26)
 $G_X(\bar{R}, \bar{R}_o) = \exp(ik_s |\bar{R}-\bar{R}_o|)/[4\pi |\bar{R}-\bar{R}_o|]$

and where S_o is the surface of the scatterer, n represents the normal to the surface and \bar{R} denotes a vector quantity. The integrals in Eqs. 25 when evaluated asymptotically for large $k_d a$ (or $k_s a$) by means of stationary

phase, yield the specularly scattered field for either bistatic or monostatic conditions. The values for the normal derivatives of the potentials evaluated at the surface are obtained from reflection coefficients associated with the corresponding planar scattering problem. For example, for the problem at hand, consider a plane dilatational wave incident on a free surface at angle θ_i from the normal.

$$\phi^i = \Phi \exp[i k_d (x \sin \theta_i - z \cos \theta_i)] \quad (27)$$

Both a dilatational and a distortional wave are scattered²⁴

$$\phi^s = A \Phi \exp[i k_d (x \sin \theta_i + z \cos \theta_i)] \quad (28)$$

$$\chi^s = B \Phi \exp[i k_s (x \sin \delta + z \cos \delta)]$$

$$\text{with } k_d \sin \theta_i = k_s \sin \delta \quad (29)$$

and

$$A = \frac{c_s \cos \theta_i \tan^2 2\delta - c_d \cos \delta}{c_s \cos \theta_i \tan^2 2\delta + c_d \cos \delta}$$

$$B = \frac{c_s \sin 2\theta_i}{c_d \cos^2 \delta} \frac{2c_s \cos \delta}{\cos \theta_i \tan^2 2\delta + c_d \cos \delta}$$

Therefore, from Eqs. 28

$$\partial \phi^s / \partial n = \partial \phi^s / \partial z = i k_d \cos \theta_i \phi^s$$

and

$$\partial \chi^s / \partial n = i k_s \cos \delta \chi^s$$

Thus, under Kirchhoff approximations, although mode conversion is accounted for (and neglecting multiple scattering), the scattered potentials can be

considered independently. Actually, if one limits oneself to back scattering, then symmetry considerations dictate that the exact solution as well yields no coupling.²⁵

For the problem of a plane dilatational wave incident on a spherical cavity the dilatational component of the (bistatic) scattered field is given by*

$$\phi_K^S = \Phi \cos \gamma \sin \gamma e^{-ik_d a \cos \gamma} e^{ik_d \rho / \zeta} \quad (31)$$

where $\rho = [R^2 a^2 - 2aR\cos(\gamma-\theta)]^{1/2}$

$$\zeta = \rho R \sin \gamma \sin \theta [\cos \gamma + (a/R) \sin^3 \gamma / \sin(\gamma-\theta) - \sin \gamma / \tan(\gamma-\theta)]^{1/2}$$

and

$$(R/a) \sin(2\gamma-\theta) = \sin \gamma$$

In the far-field, i.e., for $a/R \ll 1$, Eq. 31 reduces to the well known result for specular scattering (both bistatic and monostatic)

$$\frac{R\phi_K^S}{\phi^i} = -(a/2R) e^{ik(r-a\cos\theta/2)} \quad (32)$$

or

$$\left| \frac{R\phi_K^S}{\phi^i} \right| = a/2R \quad (33)$$

It is the nature of this formulation that it is easily constructed for arbitrary geometry and (locally reacting) surface impedance.

4. T-Matrix

The T-matrix formulation of scattering has significant computational advantages over other, more traditional, matrix formulations. These advantages relate to the nature of the elements of the matrix which turn out to be surface integrals exhibiting regular integrands.³ The first step in the formulation is to express the incident and scattered fields in

*This result was obtained by my colleague Dr. W. T. Ellison and represents an extension of his previous work on monostatic scattering.²⁶

terms of the appropriate eigenfunction series for incoming and outgoing waves, viz. cylindrical harmonics for two dimensional scattering problems and spherical harmonics for three dimensional problems. Then, a set of functions, f_j , is introduced which is complete but may or may not be orthogonal, on the scattering surface. This set of functions is not necessarily unique and may be chosen for analytical or computational considerations.⁴ Finally, the incident and scattered fields are expanded in terms of these functions f_j on the surface of the boundary and the appropriate boundary conditions are satisfied term by term. The T-matrix, which relates the unknown coefficients of the series representing the scattered field in terms of the known incident field, is thus derived. For completeness the procedure for scalar scattering is outlined below.

Consider three-dimensional scalar scattering and a scatterer that satisfies Dirichlet boundary conditions. The incident wave is given by

$$\phi^i(r, \theta, \phi) = \sum_n A_n \xi_n(r, \theta, \phi) \quad (34)$$

The scattered wave is represented by

$$\phi^s(r, \theta, \phi) = \sum_m B_m \eta_m(r, \theta, \phi) \quad (35)$$

For example, for axisymmetric problems

$$\xi_n(r, \theta, \phi) = j_n(k_r) P_n(\cos\theta)$$

and

$$\eta_n(r, \theta, \phi) = h_n(k_r) P_n(\cos\theta)$$

where j_n and h_n denote the spherical Bessel and Hankel functions respectively and P_n is the Legendre function. The Dirichlet condition on the boundary S_o is given by

$$\phi \Big|_{S_o} = (\phi^i + \phi^s) \Big|_{S_o} = 0 \quad (36)$$

Expanding Eqs. 34 and 35 in terms of the functions f_j and satisfying Eq. 36 yields the set of equations

$$\int [A_n(f_j, \xi_n) + B_n(f_j, \eta_n)] = 0 \quad n, j = 0, 1, \dots \quad (37)$$

(r, θ, ϕ) on S_o

$$\text{where } (u, v) = \int_{S_o} u^* v dS_o \quad (37a)$$

Using the usual notation, Eqs. 37 (truncated) may be written in matrix form

$$[\tilde{Q}] \bar{A} + [Q] \bar{B} = 0 \quad (38)$$

$$\text{where } \bar{A} = [A_1, A_2, \dots, A_N]$$

$$\bar{B} = [B_1, B_2, \dots, B_N]$$

$$[\tilde{Q}] = \tilde{Q}_{jn} = (f_j, \xi_n)$$

$$[Q] = Q_{jn} = (f_j, \eta_n)$$

Solving Eq. 38

$$\bar{B} = -[Q]^{-1} [\tilde{Q}] \bar{A} = T \bar{A} \quad (39)$$

where T defines the T -matrix which in turn defines the scattered field as given by Eq. 35.

III. THE USE OF HIGH FREQUENCY ASYMPTOTICS TO EVALUATE AND FACILITATE THE CONVERGENCE OF T-MATRIX SOLUTIONS

A. General Formulation

As indicated above, in many cases high frequency scattering solutions share the simplicity often found in low frequency formulations. For example, while in the low frequency, or Rayleigh, region only the volume, density and compressibility of a complex scatterer may be needed, in the high frequency regime, often only the local radii of curvature and reflection coefficient need be known to calculate the specular return. Thus, as is the case for low frequencies the nature of the solution to a variety of complex scattering problems tends to coalesce yielding a large number of scattering problems which is bounded at both the low and high frequency ends by known solutions. These solutions can benefit T-matrix formulations in a number of ways. First, they can provide convergence checks. These checks need not necessarily be in terms of matching amplitudes but also in the case of creeping wave solutions, the checks may be in terms of phase velocities (Eqs. 22 and 23) or, for transient problems arrival times.

Also, although only separable geometries have been considered in Section II, the asymptotic results can be extrapolated to other more complex geometries. This is straightforward for the specular return since it is a local phenomenon. However, as stated above, it is also the case, albeit somewhat more limited, for the creeping wave results by proper interpretation of the functional dependence of the creeping waves on the spatial coordinates.²⁷

Additionally, another use for these solutions is being proposed here. In particular, it is suggested that there may be computational advantages to be gained by integrating these solutions into the T-matrix formulation itself.

One possibility would be to use the high frequency solutions as an aide in choosing appropriate base functions, f_j . As mentioned earlier, the base functions, f_j , can be chosen for analytical considerations, e.g., consistency with the Helmholtz integral formulation, as well as for computational considerations, e.g., minimization of the mean square

deviation from the prescribed boundary conditions.³ In terms of this latter consideration, it would be reasonable to expect that knowledge of the nature of the high frequency behavior at the boundary should allow one to develop base functions, either in part or the complete set, which would yield computational benefits at high frequencies. Unfortunately, this approach would generally lead to frequency dependent base functions and it is not clear to the author how this could be conveniently accomplished in a general fashion. Thus, this possibility is not pursued further. However, what is suggested for further study is the following.

Consider the T-matrix formulation as presented in the previous section. Let $\bar{\phi}_s$ represent the (known) high frequency asymptotic solution for the scattered field which, like the actual field, can be expanded in terms of two or three dimensional harmonics for outgoing waves.

$$\bar{\phi}_s = \sum_m c_m n_m(r, \theta, \phi) \quad (40)$$

with

$$c_m = [\bar{\phi}_s, n_m] / [n_m, n_m] \quad (41)$$

Thus, since n_m are complete over all space V, Eq. 35 may be written as

$$\phi^s(r, \theta, \phi) = \phi_{mod}^s(r, \theta, \phi) + \bar{\phi}_s(r, \theta, \phi) \quad (42)$$

with

$$\phi_{mod}^s(r, \theta, \phi) = \sum_m (B_m - C_m) n_m(r, \theta, \phi) \quad (43)$$

The matrix equation (Eq. 37) becomes

$$[A_n(f_j, \xi_n) + D_n(f_j, n_n)] = -(f_j, \bar{\phi}_s) \quad , \quad (r, \theta, \phi) \text{ on } S_o \quad (44)$$

where $D_n = B_n - C_n$

In matrix notation

$$\bar{D} = T \bar{A} - Q^{-1} \bar{\phi}_s \quad (45)$$

with $\bar{\phi}_j^s = (f_j, \bar{\phi}_s)$ (46)

What is accomplished by the above manipulations is that the (unavoidable) computational difficulties that are associated with the series expansion of the scattered field at high frequency have been isolated and extracted from the T-matrix. (It should be noted that this approach is equally applicable to the wave harmonic formulation for separable geometries.)

B. Illustrative Examples

1. Spherical Cavity

To illustrate the concepts discussed in Section A we first continue our consideration of scattering from a spherical cavity and in particular, backscattering. For simplicity, we will limit our high frequency asymptotic solution to the specular return given in Section II.B.3. In other words, let $\bar{\phi}_s$ be given by Eq. 31. Further, since for a spherical scatterer, nothing is gained by choosing the set f_j to be other than the Legendre functions $P_j(\cos\theta)$. Results for the backscattered pressure and relative phase vs. frequency are shown in Figs. 2 and 3. The exact solution was obtained by summing the wave harmonic series (Eqs. 7-10), or equivalently the T-matrix series (Eqs. 35 and 37), to convergence. Roughly speaking, for the problem at hand convergence requires $N \geq 2(ka+1)$. The dashed line connects points which represent the contribution of the first term in the T-matrix series which was calculated using only a 2×2 matrix. Obviously the result is adequate only for low values of ka . The dotted line is the corresponding result for the modified T-matrix formulation (Eq. 42). Further improvement could be obtained by including the creeping wave (Eq. 22), as well as the specular, contribution to $\bar{\phi}_s$.

2. Prolate Spheriodal Cavity

The example of a spherical scatterer is of somewhat limited value as an illustrative example in the sense that the T-matrix approach degenerates identically to the wave harmonic solution. Thus, in this section we consider (scalar) scattering from a cavity in the shape of a

prolate spheroid. For convenience, we again limit ourselves to back-scattering and consider end-on incidence (Fig. 4). The prolate spheroidal coordinates (ξ, n) are related to cartesian coordinates by the transformation

$$\begin{aligned} x &= (d/2) \left[(1-n^2)(\xi^2-1) \right]^{1/2} \\ z &= (d/2)n\xi, \end{aligned} \quad (47)$$

with $-1 \leq n \leq 1$ and $1 \leq \xi < \infty$

The scattering surface is defined by the equation $\xi = \xi_0$. For the present problem ξ_0 is taken to be 1.1547, which yields a spheroid with a 2:1 aspect ratio. For this geometry, and assuming symmetry about z , the inner product (Eq. 37a) becomes

$$(u, v) = 2\pi(d/2)^2 (\xi_0^2 - 1)^{1/2} \int_{-1}^1 (u^* r) (\xi_0^2 - n^2)^{1/2} dn \quad (48)$$

Also, the local radius of curvature at $(\xi_0, 1)$, i.e., end-on, is given by

$$a^* = (d/2) (\xi_0^2 - 1) / \xi_0 \quad (49)$$

Thus, the high frequency (Kirchhoff) backscattered level (equivalent to Eq. 33 for the spherical scatterer) is given by

$$|R\phi_K^S/\phi_i^I| = a^*/2R \quad (50)$$

A comparison between this asymptotic result and the exact solution²⁹ is shown in Fig. 5. In order to maintain a notation consistent with Reference 29 the ordinate in Fig. 5 is given in terms of a backscattered cross-section which is defined by

$$\sigma/\sigma_k = [2R/(d/2)] [\xi_0 / (\xi_0^2 - 1)] [\phi_S/\phi_i]^2 \quad (51)$$

Also shown in Fig. 5 is the result of a T-matrix formulation using base functions

$$f_j = \cos(j\theta) \quad j = 0, 1, \dots N \quad (52)$$

where

$$\theta = \tan^{-1}(x/z) = \tan^{-1} \{ [(1-\eta^2)(\xi_0^2 - 1)]^{1/2} / (\eta \xi_0) \} \quad (53)$$

Consistent with the previous example the number of terms required for convergence is given by

$$N \geq 2(k\xi_0 d/2 + 1) \quad (54)$$

The integration implied by Eq. 48 was performed using the trapezoid rule with a mesh size equivalent to $\lambda/8$.

It should be noted that, as was the case in the previous section, the high frequency asymptotic solution is reached before the convergence criterion (Eq. 54) becomes prohibitive. An indication of the effectiveness of the high frequency modification for this case is shown in Fig. 6. Here the percent error incurred by constructing the scattered field using only the first $N/2$ terms in the T-matrix solution is plotted vs non-dimensional frequency for the modified as well as the unmodified formulation.

In summary, both examples, although elementary, indicate that the extraction of appropriate high frequency components from acoustic (or elastic) scattering problems may represent a viable means for improving the convergence of T-matrix formulations to more complex problems.

REFERENCES

- 1 Y. H. Pao and V. Varatharajulu, "Huygen's Principle, Radiation Conditions, and Integral Formulas for the Scattering of Elastic Waves," J. Acoust. Soc. Am. 59, 1361-1371 (1976).
- 2 P. C. Waterman, "New Formulation of Acoustic Scattering", J. Acoust. Soc. Am. 45, 1417-1429 (1969).
- 3 W. M. Visscher, "A New Method for Calculating Elastic Wave Scattering by a Flaw", First International Symposium on Ultrasonic Materials Characterization, June 7-9, 1978 (National Bureau of Standards, Gaithersburg, MD).
- 4 V. K. Varadan, V. V. Varadan, and Y. H. Pao, "Multiple Scattering of Elastic Waves by Cylinders of Arbitrary Cross-Section: SH Waves", J. Acoust. Soc. Am. 63, 1310-1319 (1978).
- 5 G. Kristensson and S. Strom, "Scattering from Buried Inhomogeneities--A General Three Dimensional Formalism", J. Acoust. Soc. Am. 64, 917-936 (1978).
- 6 R. L. Weaver and Y. H. Pao, "Application of the Transition Matrix to a Ribbon-shaped Scatterer", J. Acoust. Soc. Am. 66, 1199-1206 (1979).
- 7 A. Bayliss and L. Maestrallo, "Measurements and Analysis of Far-field Scattering from a Prolate Spheroid", J. Acoust. Soc. Am. 64, 896-900 (1978).
- 8 P. M. Morse and K. U. Ingard, "Linear Acoustic Theory", Encyclopedia of Physics, edicted by S. Flugge, Marbur, Volume VI/1 (Springer-Verlag, Berlin, 1961) pp. 23-24.
- 9 Y. H. Pao and C. C. Mow, Diffraction of Elastic Waves and Dynamic Stress Concentrations, (Crane Russak, New York, 1973) Ch. 6.

- 10 G. N. Watson, Proc. Royal Soc. (London) Ser. A 95, 83-99 (1918).
- 11 E. C. Titchmarsh, Introduction to the Theory of Fourier Integrals, 2nd ed., (Oxford University Press, London, 1937) p. 60.
- 12 M. Nagase, "On the Zeroes of Certain Transcendental Functions Related to Hankel Functions, Parts I and II", J. Physical Soc. of Japan 9, 5, Sept.-Oct. 1954, p. 826-853.
- 13 M. Nagase, "Diffraction of Elastic Waves by a Spherical Surface", J. Physical Soc. of Japan 11, 3, March 1956, pp. 279-301.
- 14 M. Abramowitz and I. A. Stegun, Handbook of Mathematical Functions, (NBS, Supt. of Documents, Washington, D.C., 1964) Ch. 10.
- 15 F. R. Norwood and J. Miklowitz, J. Appl. Mech. 34, Trans. Amer. Soc. Mech. Eng. Ser. E 89, (1967) 735-744.
- 16 J. Miklowitz, "Scattering of a Plane Elastic Compressional Pulse by a Cylindrical Cavity", Applied Mechanics, Proceedings of the 11th International Congress of Applied Mechanics (Munich, 1964).
- 17 J. C. Peck, Plane Strain Diffraction of Transient Elastic Waves by a Circular Cavity, Ph.D. Thesis, Calif. Inst. of Tech., June 1965.
- 18 G. C. Gaunaurd and H. Uberall, "Theory of Resonant Scattering from Spherical Cavities in Elastic and Viscoelastic Media", J. Acoust. Soc. Am. 63(6), June 1978, pp. 1699-1712.
- 19 G. C. Gaunaurd and H. Uberall, "Numerical Evaluation of Modal Resonances in the Echoes of Compressional Wave Scattered from Fluid-filled Spherical Cavities in Solids", J. Physics 50(7), July, 1979, pp. 4642-4660.
- 20 D. Brill, G. Gaunaurd, and H. Uberall, "Response Theory of Elastic Shear-Wave Scattering from Spherical Fluid Obstacles in Solids", J. Acoust. Soc. Am. 67(2), Feb. 1980, pp. 414-424.
- 21 J. W. Crispin, Jr. and K. M. Siegel, Methods of Radar Cross-Section Analysis, (Academic Press, New York, 1968).

- 22 W. G. Neubauer, "A Summation Formula for Use in Determining the Reflections from Irregular Bodies", J. Acoust. Soc. Am. 35, 279-285 (1963).
- 23 M. C. Junger and D. Feit, Sound, Structures, and Their Interaction (MIT Press, Cambridge, MA, 1972) Ch. 11.
- 24 L. M. Brekhovskikh, Waves in Layered Media, (Academic Press, New York, 1960) Ch. 4.
- 25 B. R. Tittmann, "Mode Conversion and Angular Dependence for Scattering from Voids in Solids", Ultrasonics Symposium Proceedings, IEEE Cat. # 75 CHO 994-45U (1975).
- 26 W. T. Ellison, The Effectiveness of Finite Impedance Strip Coatings (U), CAA Confidential Report C-467-210 prepared for ONR, Code 212, under Contract N00014-69-C-0096, January 1975.
- 27 D. Feit, "High Frequency Response of a Point Excited Cylindrical Shell", J. Acoust. Soc. Am. 49(5) (May 1971) pp. 1499-1504.
- 28 C. Flammer, Spheriodal Wave Functions, (Stanford University Press, Stanford, CA, 1963).
- 29 J. J. Bowman, T. B. A. Senior and P. L. E. Uslenghi, Electromagnetic and Acoustic Scattering by Simple Shapes (North-Holland Publishing Company, Amsterdam, 1969) Ch. 11.

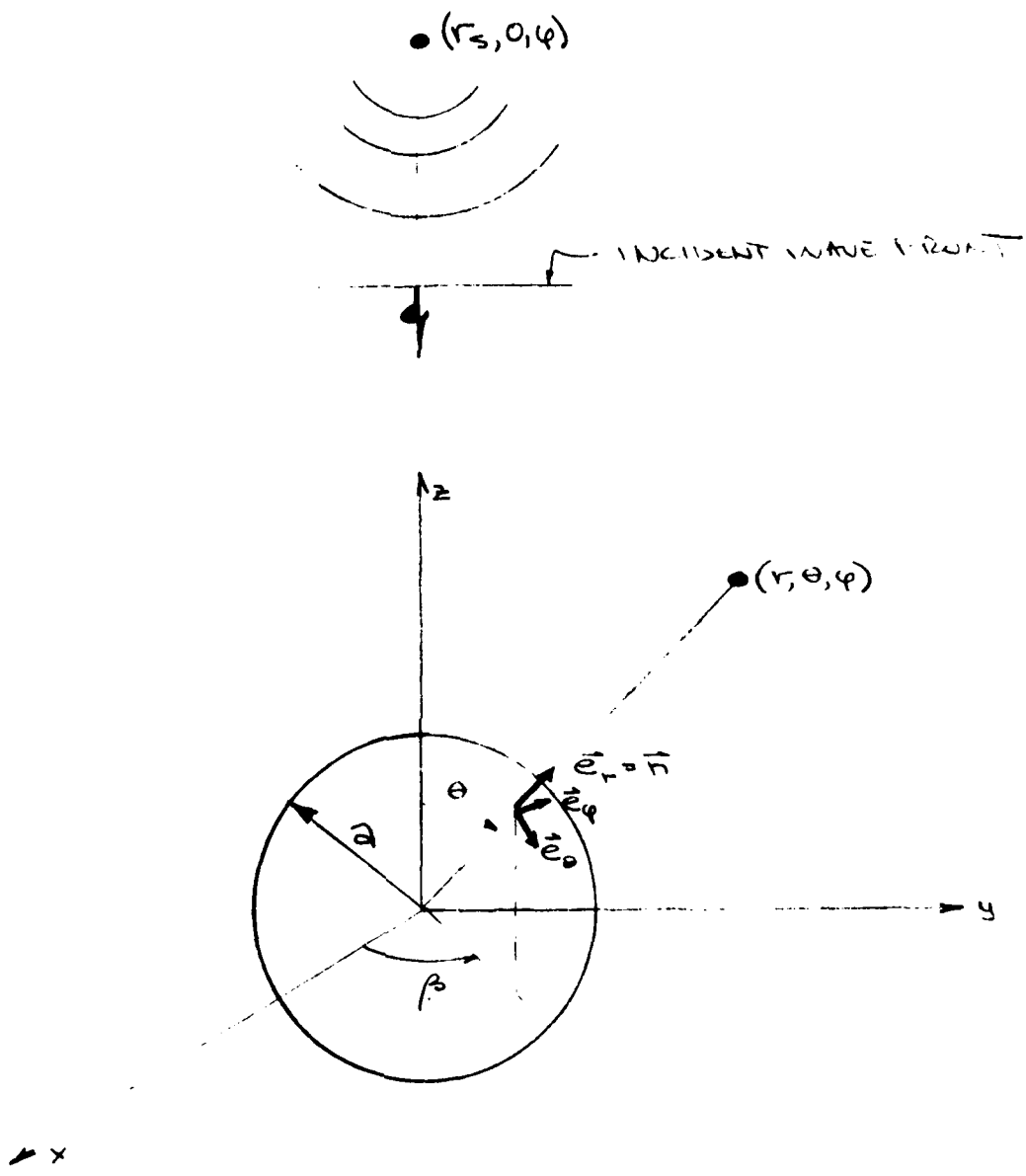


Fig. 1 - Geometry for Scattering from Spherical Inclusion

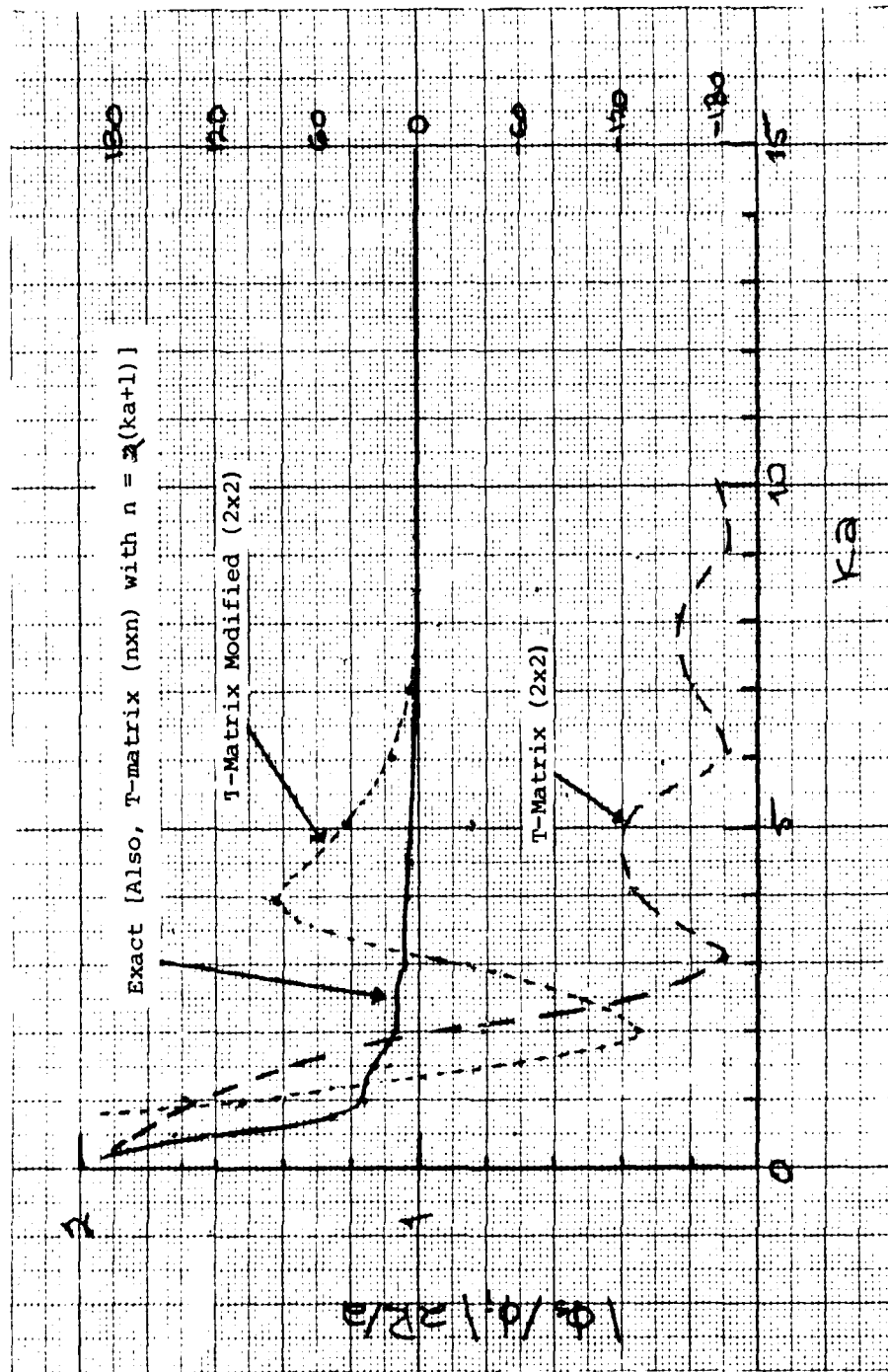


Fig. 2 - Magnitude of Backscattered Potential From a Spherical Cavity vs. ka :
Effect of High Frequency Modification to T-Matrix Formulation.

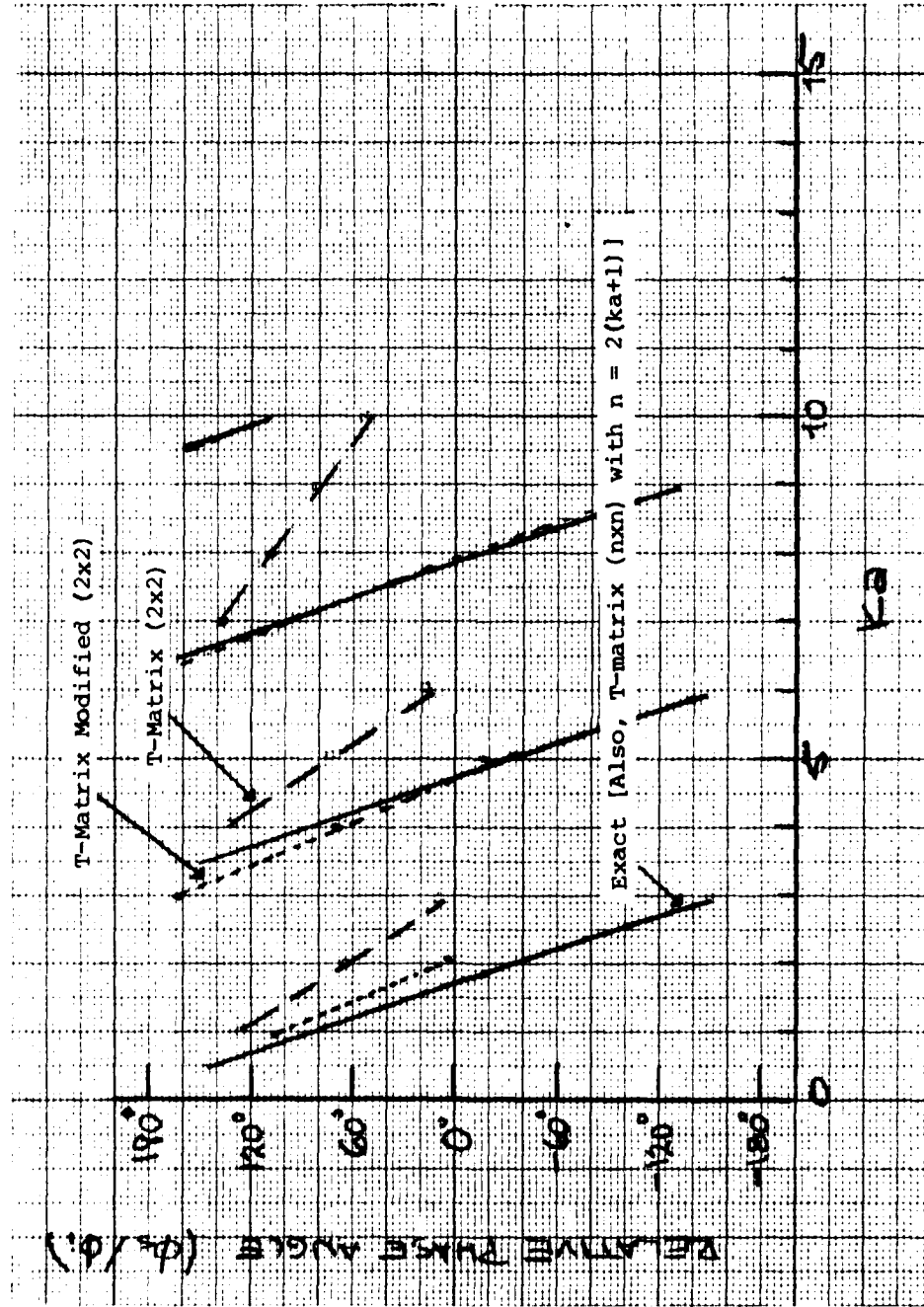


Fig. 3 - Relative Phase of Backscattered Potential from a Spherical Cavity vs. ka :
Effect of High Frequency Modification to T-Matrix Formulation.

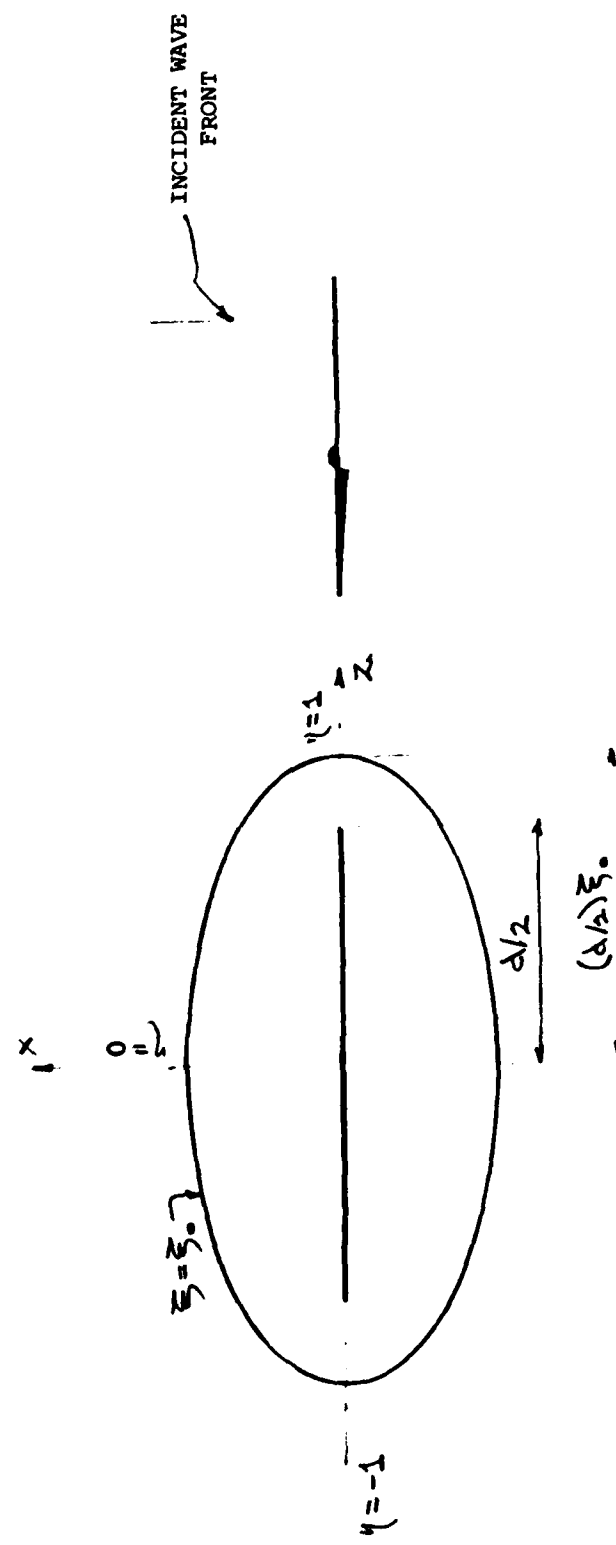


Fig. 4 - Geometry for Scattering from Prolate Spheroid.

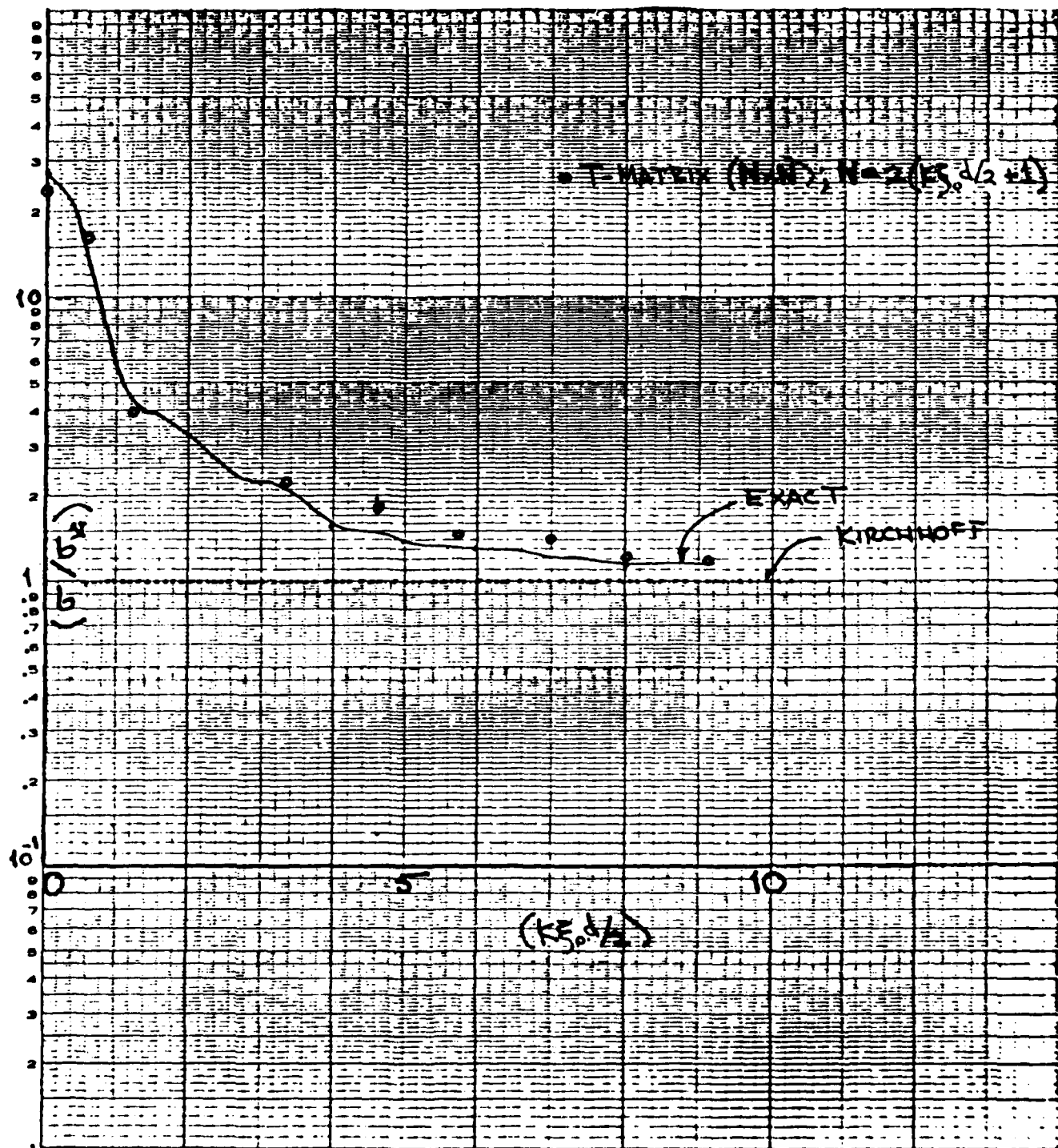


Fig. 5 - Magnitude of backscattered cross-section from a prolate spheriodal cavity vs $k^2 d/2$.

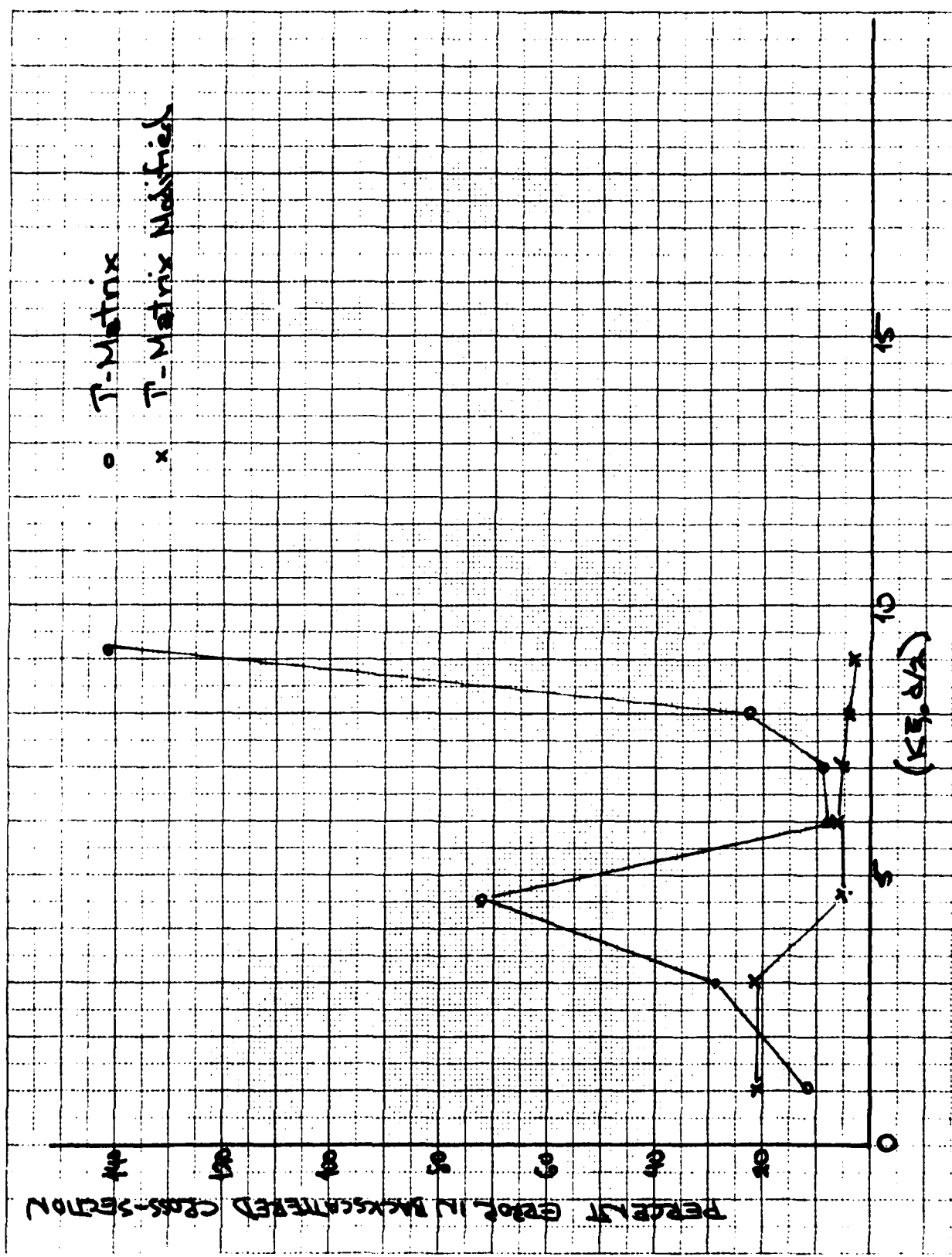


Fig. 6 - Percent error in backscattered cross-section for a prolate spheroidal cavity using $N/2$ terms for ϕ_s (N given by Eq. 54).

